Biosystems Engineering (2005) **90** (2), 173–184
doi:10.1016/j.biosystemseng.2004.11.001
PM—Power and Machinery

Effect of Air-jet Configuration on Spray Coverage in Vineyards

B. Panneton; B. Lacasse; M. Piché

Agriculture and Agri-Food Canada, Horticultural Research and Development Centre; 430 Boul. Gouin, St-Jean-sur-Richelieu, Qué., Canada J3B 3E6; e-mail of corresponding author: pannetonb@agr.gc.ca

(Received 26 March 2004; accepted in revised form 15 November 2004; published online 4 February 2005)

A new type of sprayer developed for orchard is being adapted for vine spraying. The technology uses vertical air sleeves, generating a two-dimensional horizontal air jet, to distribute spray droplets within the canopy. Three different configurations were tested to determine the combination which provides the most appropriate spray distribution within the canopy along with the highest coverage on artificial cylindrical targets. One configuration (a) used a single air jet perpendicular to the row. Two other configurations used a pair of sleeves, one sleeve on each side of the row. In configuration (b), airflow rate was distributed evenly between the two sleeves. In configuration (c), the distribution of air was varied along with the angle of attack, providing an interaction between the two airflows. Coverage on 22 mm cylindrical targets covered with water-sensitive papers was evaluated across the vine rows. These papers were processed using image analysis. Results showed that coverage was maximised using configuration (c). The use of a pair of sleeves, in configurations (b) and (c), provided a more uniform distribution of droplets locally.

1. Introduction

Criticisms of pesticide use are numerous but it is expected that farmers will continue to rely on chemical control because it is the most cost effective and rapid way of minimising crop losses due to weeds, pathogens and insects. In this context, restricting pesticides as far as possible to the actual target is fundamental to proper pest management (Matthews, 2000b) and this is where pesticide application technologies have a key role.

In vineyards, a wide range of technologies is being used for applying pesticides (Matthews, 2000b; Viret *et al.*, 2003) manually operated sprayers, knapsack mist blowers, directed nozzle hydraulic sprayers, air blast sprayers, over-row sprayers, tunnels with or without air-assistance as well as aerial applications. While debatable, it is generally accepted that the sprayer should uniformly deposit material on the plants (Furness & Pinczewski, 1985; Pergher *et al.*, 1997b; Stafford *et al.*, 1970). Appropriate use of air-assistance is required to improve the distribution of deposits and collection efficiency of plant parts (Matthews, 2000a). At the leaf scale, a better balance between coverage of the upper and lower surfaces requires some form of air-assistance (Viret *et al.*, 2003). At a larger scale, spray partition within the canopy is affected by airflow rate (Pergher & Gubiani, 1995) and air speed (Randall, 1971) as well as the orientation of the airflow and the number of air outlets used to direct the air and the spray to the canopy (Furness & Pinczewski, 1985; Gohlich, 1985; Pergher *et al.*, 1997a; Pezzi & Rondelli, 2000).

Proper use of air-assistance is not straightforward as a too strong or a too weak air jet may cause inadequate deposit, uneven distribution within canopy and increased environmental contamination (Doruchowski *et al.*, 1997). For the same amount of power, a higher airflow rate at a lower air speed penetrated trees better and produced better leaf coverage than lower volumes of higher velocity air (Randall, 1971). This held true provided than the air speed was high enough to form openings in the canopy for the air stream to penetrate. For Cox apple trees, a minimum air speed of 12·2 m/s was sufficient. More air does not automatically imply better coverage as on dwarf apple trees. Total deposit was better using a lower airflow rate while for a higher airflow rate, the amount of spray blown through the

Notation

A	sampling surface area, mm
C	mean coverage, %
C_2	coverage that would correspond to C when the application volume is doubled, %
$\widehat{C}$	corrected coverage, %
$\tilde{C}_{Ci,j}$	deviation of the co-variable from its mean value associated with treatment, %
d	droplet diameter, mm
k	constant depending on the spread factor of the droplet of the sampling surface
n	number of droplets
p	probability
Q_i	effect of airflow rate for treatment i, %
Q_s	specific airflow rate, %
Q_v	total airflow rate through the fan, m^3/s
R	airflow balance, %
v	travel speed, m/s
V	air speed, m/s
V_i	effect of air speed for treatment i, %
V_v	canopy volume per unit length of row, m^3/m
x_c	distance required for C to fall to 36·8% of its initial value C_0, m
β	slope of the linear regression between the co-variable and $C_{i,j}$
ε	error term
μ_C	overall mean coverage, %

Subscripts

i	treatment
j	replicate

canopy was increased (Holownicki *et al*., 2002). These results were reproduced when wind speed was low but in higher wind speeds, mean deposits were lower at the lowest airflow rate (Cross *et al*., 2003). Leaf fluttering is enhanced by increasing turbulence in the airflow and this could be used to increase droplet collection by the foliage. In this regard, high air speed is detrimental as it decreases fluttering (Matthews, 2000b). The type of fan and the shape of the resulting air jet should also be considered. Air speed decays more slowly from a cross-flow fan which produces a two-dimensional jet (Abramovich, 1963) and it was demonstrated that directed air jet sprayers with a converging flow resulted in higher deposits and lowest spray loss even when the flow rate was decreased by a factor of three (Doruchowski *et al*., 1996).

A new type of spray recovery sprayer, initially developed for apple orchards (Panneton *et al*., 2001) is being adapted to vine spraying in our laboratory. This sprayer uses vertical air sleeves to distribute a droplet-laden airflow along the full height of the canopy. It also uses a porous air-droplet separator on the opposite side of the vine to catch the droplets not retained by the foliage. As a preliminary phase of the design, a series of experiments has been performed to evaluate the potential of three basic configurations: one using a single sleeve-separator unit, one using a pair of sleeve-separator units mounted at 180° with respect to each other and a last one using two sleeves and a single air-droplet separator panel. The objective of the study was to identify the best configuration of air jets to optimise spray penetration inside the canopy and spray deposition uniformity across the canopy.

2. Materials and methods

The experimental sprayer was designed in such a way that it could serve as a test bench for the three configurations [(a), (b) and (c) configurations]. Airflow was provided by a centrifugal fan. The fan exit was fitted with a Y-section to divide the flow in two streams. An adjustable internal baffle was used to choke the fan output to control the total airflow. Another adjustable internal baffle was used to balance the airflow between the two branches of the Y-section. The entrance port on the fan was fitted with a tube terminated by a bell mouth [*Fig. 1*(*a*)]. The tube was 254 mm in diameter and 1016 mm long. At 508 mm from the entrance of the tube a pair of flow meters (Debimo-254, Kimo, France) was installed and connected to two differential manometers (Magnehelic® Series 2000) in parallel. The flow meters were 432 mm upstream from the fan housing. Distances upstream and downstream from the flow meters were set according to AMCA (1990). For low airflow rates, a manometer with a 0–50·8 mm H_2O range was used and a 0–254 mm H_2O range covered the higher airflow range.

For all configurations, the air was brought to the vertical air sleeves using a flexible tube, 254 mm in diameter. The top of the vertical sleeve was aligned with the top of the canopy and it extended downwards to stop at about 254 mm above the ground. The cross-section of the vertical sleeves decreased linearly from top-to-bottom to make sure that the exit air speed was constant along the full height. The air exit was a slot of constant width extending the full length of the sleeve (1000 mm). The slot geometry was defined using two tubes, 25·4 mm in diameter. The distance between the two tubes or the slot width was adjusted to provide an

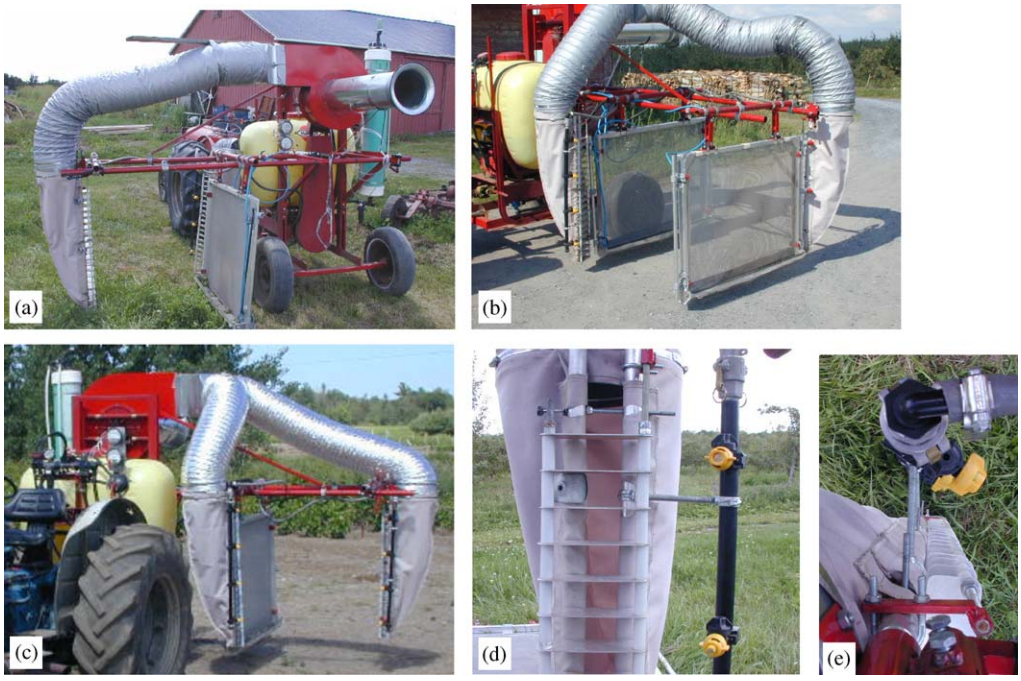

Fig. 1. Experimental prototype: (a) one air sleeve facing one air-droplet separator; (b) two air sleeves, each one pointing to an air-droplet separator; (c) two air sleeves, one pointing towards the air-droplet separator and the other one intersecting the first air stream at the centre of the row; in (a), the long pipe extending from the fan axis is the entrance port where total airflow to the fan is measured; (d) and (e) geometry of the air exit and location of nozzles

independent control of airflow rate and air speed [*Fig. 1*(*d*)]. With such a sleeve design, air escapes the sleeve with a significant downward velocity (Panneton *et al.*, 2001). To force the exit air to move parallel to the ground, a series of fixed baffles were installed immediately in front of the exit slot. These were large enough to cover the range of slot width actually used during the experiments and were 50·8 mm long.

The spray nozzles were installed next to the air exit slot [*Fig. 1*(*d*)] on a wet boom. The first nozzle at the bottom of the boom was at about 381 mm above the ground and nozzle spacing was 254 mm. Four nozzles were used with each sleeve. The exit of the nozzle was aligned with the exit of the flow straightening baffles [*Fig. 1*(*e*)] and at 114 mm from the border of the air exit slot. The nozzles were set at an angle of 30° with respect to the jet axis. At this angle, most, if not all the spray, penetrated and was entrained by the air jet. The nozzles were TX-VS3 hollow cone nozzles (Spraying Systems Co, Wheaton, Il) operated at 345 kPa. Under these conditions these nozzles generated a fine spray (ASAE, 2000) and the application rate was 25 *l*/ha per boom.

The design of the air-droplet separator was the same for all configurations. It was a rectangular frame, 1200 mm wide by 1000 mm high (inside dimensions) holding two screens, at 16 mm one from the other. Each screen had a 66% opening area ratio.

The three configurations are illustrated in *Fig. 1* and their geometric details are provided in *Fig. 2*. For configuration (a), the lateral distance between the vine and the air sleeves or the air-droplet separator panels was constant at 270 mm. For configurations (b) and (c), the distance to the vine was 320 mm on both sides. Configuration (a) used one air sleeve and one air-droplet separator facing each other, the separator being on the sprayer side of the row. The jet axis was offset forward to compensate for the forward motion of the sprayer. In configuration (b), a symmetrical pair of air sleeve and air-droplet separator was used. The axis of the two air jets were parallel and were pointing straight at the centre of the separator panel on the other side of the row. The exit of the two air sleeves were at a distance of 1500 mm along the row of vine. Configuration (c) used two air sleeves and a single air-droplet separator. The sleeve away from the sprayer was pointing at the centre of the separator panel. The sleeve on the tractor side was installed in front of the separator and was pointing at the intersection between the axis of the other jet and the axis of the row of vine.

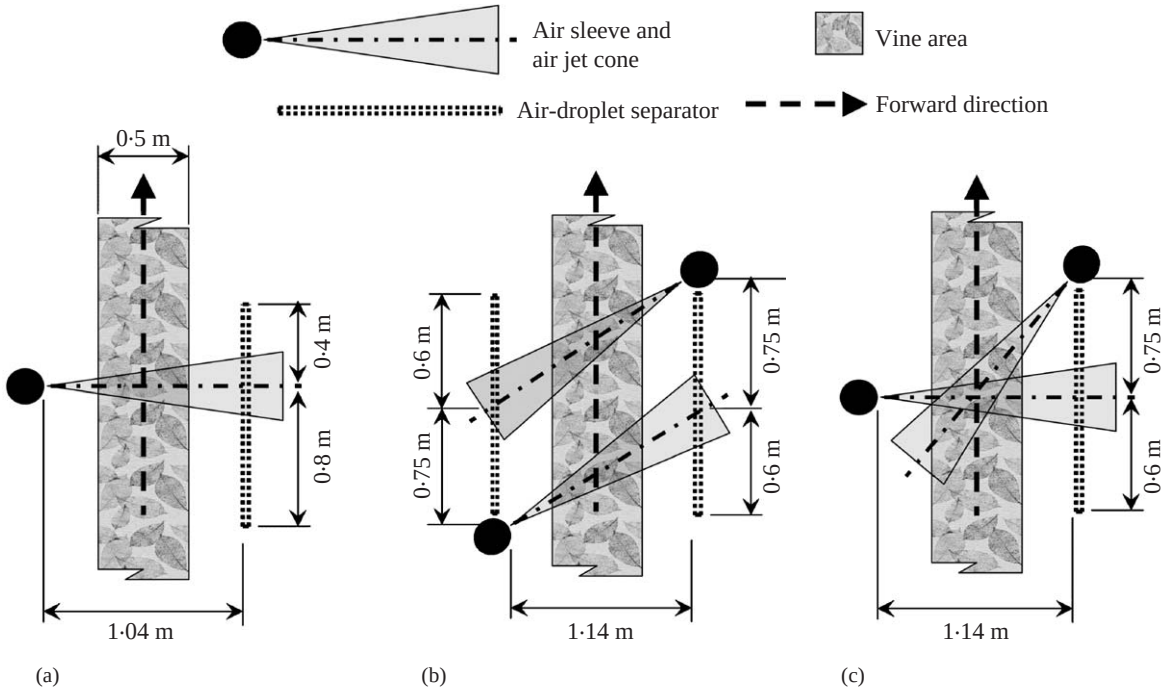

Fig. 2. Detailed geometry of the three configurations

Table 1
Value of the independent variables

Configuration		*Air speed, m/s*	*Specific flow rate, %*	*Flow rate balance*	*Slot width, mm*	
					Sprayer side	*Far side*
(a)		15·0	62·5			50
		15·0	125			100
		30·0	62·5			25
		30·0	125			50
	Reference	22·5	94			50
(b)		15·0	62·5	50–50	28	28
		15·0	125	50–50	55	55
		30·0	62·5	50–50	14	14
		30·0	125	50–50	28	28
	Reference	22·5	94	50–50	28	28
(c)		15·0	62·5	30–70	16	38
		15·0	62·5	40–60	21	32
		15·0	125	30–70	32	75
		15·0	125	40–60	43	64
		30·0	62·5	30–70	8	19
		30·0	62·5	40–60	11	16
		30·0	125	30–70	16	38
		30·0	125	40–60	21	32
	Reference	22·5	94	35–65	19	35

For each configuration, spray penetration and coverage were measured on water-sensitive papers (Spraying Systems, Wheaton, Il) for different combinations of air speed and airflow rate. For configuration (c), the airflow rate balance between the two air sleeves was also used as an independent variable. A full factorial experimental plan was used with three replications. The experimental scenario is summarised in Table 1. The air speed was

measured directly at the exit slot of the vertical sleeves. The airflow rate was expressed as a specific flow rate defined by

$$Q_s = \frac{100 \times Q_v}{V_v \times v} \quad (1)$$

where: Q_s is the specific airflow rate in %; Q_v is the total airflow rate through the fan in m^3/s; V_v is the canopy volume corresponding to 1 m along the row in m^3/m; and v is the travel speed in m/s. To compute V_v, the treated cross-section was considered as the space from the top to the bottom of the vertical sleeve (1000 mm) and laterally from the air-droplet separator front surface to the exit slot [1·04 m for configuration (a) and 1·14 m for configurations (b) and (c)]. The travel speed was maintained at 1·17 m/s (4·2 km/h) for all tests. A specific flow rate of 100% corresponds to a combination of fan output and travel speed such as to replace all the air in V_v with the droplet-laden airflow from the sprayer. The flow rate balance of configurations (b) and (c) defined the proportions of the air volume delivered on each side of the row. The first number is the fraction of the total flow emitted on the sprayer side.

For each configuration, a set of reference conditions was defined (Table 1). These were used to perform reference runs. The coverage data from these reference runs were used as co-variables (Neter *et al*., 1990) in the analysis of variance (Unistat, 2002). Using co-variables permitted to account for day-to-day variations in the field conditions (canopy development, air temperature and humidity, *etc*). In addition, the amplitude of these variations was limited in two ways. Firstly, the experiment started only after the first time the canopy has been trimmed to a known height (1·2 m) and width (0·5 m). In Quebec, mechanical trimming is done on a regular basis, keeping the canopy volume fairly constant over time. Secondly, experiments were not performed if the mean wind speed (5 min average) recorded on site (Young propeller anemometer, model 5107) exceeded 3 m/s. At the beginning of each trial day, a first reference run was performed. During the day, a new reference run was performed whenever the average wind speed changed by more than 1 m/s or the wind direction changed by more than 45°.

Before each run, the slot widths were adjusted. Then the total airflow rate was adjusted using the appropriate adjustable baffles and readings of the airflow meter. In the case of configuration (c), the other adjustable baffle was set to the appropriate position to divide the flow as required. These adjustments were previously defined during preliminary tests. As a final check, the air speed at the sleeve exit was measured using a Pitot tube. Adjustments were modified until air speeds were within 10% of their target value.

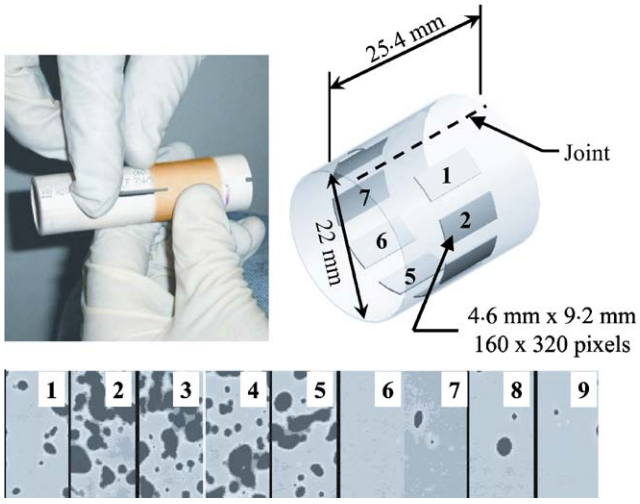

Fig. 3. Water-sensitive sampling tubes; top left, insertion of metal clip; top right, tube geometry and location of image analysis windows; bottom, unrolled sequence of 9 images from a single tube where number on the images correspond to number on the tube drawing

Sampling was performed by deploying arrays of water-sensitive tubes (*Fig. 3*). Tubes were used because sampling is not sensitive to local airflow direction projected in the plane perpendicular to the tube axis. Tube axis was set vertical. Strips of water-sensitive paper were wrapped around polyvinyl chloride (PVC) tubes (22 mm diameter) and held in place with a metal clip near the joint (*Fig. 3*). Supports holding three tubes were installed so that one tube was aligned with the centre of the row of vine and the other two tubes where just at the outer limits of the vine canopy. The tube midpoint was at 600 mm above ground. The joint in the sampling tubes (*Fig. 3*) was always oriented facing the direction 180° from the travel direction of the sprayer. A total of six tube supports were deployed at random locations along two adjacent rows of vine (3 per row). The two rows were sprayed travelling in opposite direction to remove any bias from the wind direction. For each experiment, a total of 18 sampling tubes were necessary. Great care was taken to maintain the environment of the tubes as dry as feasible. Tubes were always manipulated wearing latex gloves. Except during the actual experiment, tubes were placed in sealed box with a pocket of desiccant. As a result, the contrast between stained areas and background of the water-sensitive paper was always excellent.

Image analysis of sampling tube was performed to extract the surface of the stained area using a procedure developed previously (Panneton, 2002). A motorised sample holder was constructed. By rotating the sample in front of a camera, a series of nine images were grabbed for analysis (*Fig. 3*). Each image represented an

area of 4·6 mm by 9·2 mm at a resolution of 28·8 μm per pixel. For each image, the percentage of the area that was stained by water was measured. This variable will be referred to as the coverage in this paper. Each image is centered in a 36° sector on the cylinder and no image was acquired at the joint location. Image numbers (1–9) identify a unique angular location.

The application volume was 25 *l*/ha for configuration (a) and 50 *l*/ha for configurations (b) and (c). For comparing configuration (a) to the others, coverage data for configuration (a) were corrected following an approximate extension of the equation relating coverage to the number of impacts of droplets of a known diameter on a surface (Spillman, 1987):

$$C = \left[1 - \exp\left\{\frac{kd^2n}{A}\right\}\right] \times 100 \qquad (2)$$

where: C is the mean coverage in %; k is the constant depending on the spread factor of the droplet of the sampling surface; d is the droplet diameter in mm; n is the number of droplets; and A is the sampling surface area in mm^2.

To apply Eqn (2), two hypotheses are required: (1) Eqn (2) applies approximately to a polydisperse spray replacing kd^2 with a suitable constant; and (2) when the application volume changes, the droplet spectra remains the same which is our case as the doubling in the application volume resulted solely from doubling the number of nozzles. Applying these two hypotheses, Eqn (2) can be used to write

$$C_2 = 2C - C^2 \qquad (3)$$

where C_2 is the coverage that would correspond to C when the application volume is doubled.

3. Results and discussion

The range of meteorological conditions encountered during the experiments was narrow. Five minute averaged wind speeds were in the range from 1 to 2 m/s for 84% of the experiments and the maximum air speed was 2·27 m/s. Wind direction was more variable. It was within 45° from the perpendicular to the rows of vine 62% of the time.

Data were visualised using polar plots (*Fig. 4*). Each of the four graphs in *Fig. 4* presents mean coverage for a set of independent variables. Mean values were computed by averaging the six coverage values available for each angular position (1–9) at a fixed lateral position with respect to the vine (sprayer side, centre and far side). Data for angular position 0 were computed using a linear interpolation between mean coverage at positions 1 and 9. Position 0 was on the joint of the water-sensitive paper cylinder and this position was facing the tractor as it came towards the sampler. The

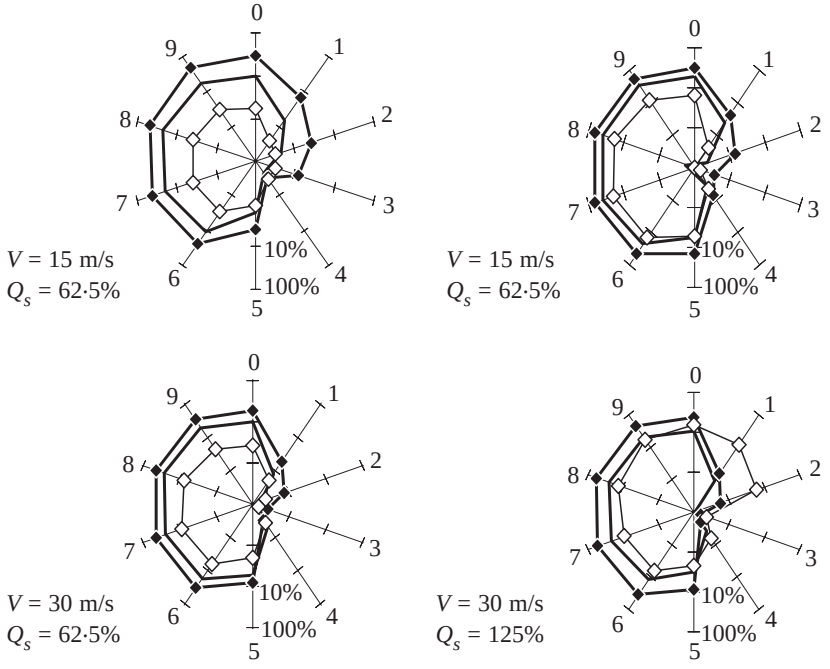

Fig. 4. Polar plots of coverage for configuration (a); coverage values corrected to double application volume for visual comparison with Fig. 7; V, air speed; Q_s, specific airflow rate; —, centre; —◆—, far side; —◇—, sprayer side

tractor can be seen as moving from top-to-bottom and passing on the right-hand side of the graphs. On the graph, coverage increases with radius following a logarithmic scale. For configuration (a), it is immediately visible from the graphs that increasing the airflow rate did increase coverage at all locations but most notably on the sprayer side (away from the air source). Increasing the air speed did not increase coverage to the same extent. As doubling either the airflow rate or the air speed doubles the amount of energy required to move the air, the results showed that increasing airflow rate would be a better choice than increasing air speed for improving coverage. The profiles are slightly tilted as could be expected since the resultant air stream was moving in a direction resulting from the addition of the travel speed of the sprayer and the exit velocity of the air. This last component was decreasing rapidly with distance from the exit due to jet diffusion. The profile amplitudes dropped rapidly on the back side of the cylinders (face not exposed to the coming airflow). This is an indication that the level and the scale of turbulence in the flow were not large enough to promote deposition on surfaces sheltered from the airflow.

Data were transformed according to the linear model that takes into account the effect of the co-variable. The basic linear model was

$$C_{i,j} = \mu_c + Q_i + V_i + Q_i V_i + \beta \tilde{C}_{Ci,j} + \varepsilon_{i,j} \qquad (4)$$

where: $C_{i,j}$ is the mean coverage for treatment i and replicate j; μ_C is the overall mean coverage; Q_i is the effect of airflow rate for treatment i; V_i is the effect of air speed for treatment i; $Q_i V_i$ is the interaction; β is the slope of the linear regression (least-squares method) for $C_{i,j}$ with $C_{Ci,j}$ as the independent variable, $\tilde{C}_{Ci,j}$ is the deviation of the co-variable from its mean value associated with treatment i; and $\varepsilon_{i,j}$ is the error term. The mean coverage was the average of the coverage values from a single tube. Prior to averaging, data from image 5 was removed to maintain sampling symmetry around the tube as no data was available over the joint in the sampling tube. The slope β was the slope of the linear regression. The corrected coverage $\hat{C}_{i,j}$ was defined as

$$\hat{C}_{i,j} = C_{i,j} - \beta \tilde{C}_{Ci,j} = \mu_C + Q_i + V_i + Q_i V_i + \varepsilon_{i,j} \qquad (5)$$

Equation (5) was the basis for the analysis of variance. A plot of the corrected coverage (*Fig. 5*) showed the same trends as on *Fig. 4*. The analysis of variance revealed that the effect of airflow rate was significant for the centre (probability $P = 0{\cdot}02$) and on the far side from the sprayer ($P < 0{\cdot}01$). Airflow rate was less significant ($P = 0{\cdot}06$) on the sprayer side. In all cases, a higher airflow rate was associated with a larger coverage. Air speed showed significant effect in the centre ($P = 0{\cdot}05$) with a better coverage associated with a smaller air speed at high specific airflow rate.

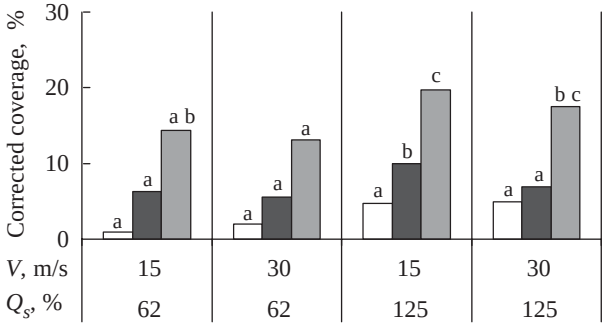

Fig. 5. Mean coverage results for configuration (a); different letters in chart represent significantly different corrected coverage within a single canopy location [least significant difference (LSD), probability $P < 0{\cdot}05$]; V, air speed; Q_s, specific airflow rate; □, sprayer side; ■, centre; ■, far side

The decay in coverage with distance from the outlet was modelled with an equation of the form:

$$C(x) = C_0 \exp\left\{\frac{-x}{x_c}\right\} \qquad (6)$$

The constant x_c is the distance required for C to fall to 36·8% of its initial value C_0. At the lower flow rate (62·5%), x_c was 0·24 m and it was 0·39 m at 125%. This decay in coverage resulted from the filtering effect of the vegetation. While the decay rate was decreased with increasing specific airflow rate, it remained significant with configuration (a).

The mean coverage computed over a single sampling tube is a measure of the total spray flux at the sampling location. The coefficient of variation of the coverage (CV) computed over a single tube (image 5 excluded) was calculated as a measure of the local coverage uniformity (*Fig. 6*). This variable then received the same statistical treatment as the mean coverage. The analysis of variance revealed that air speed and airflow rate did not induced significant changes ($P > 0{\cdot}05$) on CV.

Polar plots of the coverage for configuration (b) (*Fig. 7*) displayed more symmetrical patterns than for configuration (a) (*Fig. 4*). As expected, this effect was more pronounced in the centre of the row but noticeable differences are displayed on the sprayer and far sides. Plots are tilted by about -30° with respect to the horizontal, an angle comparable to the 33° tilt of the vertical air sleeves. Having this angle reproduced in the coverage data is an indication that there was a minimum interaction between the two air jets. A statistical treatment similar to the one applied for configuration (a), showed that on the sprayer and far sides, treatment effects on the corrected coverage were not significant ($P > 0{\cdot}05$). In the centre, the airflow rate

had a significant effect on corrected coverage, with better coverage at 125% for the higher air speed (*Fig. 8*). Airflow rate had a significant effect ($P = 0{\cdot}036$) on corrected CV on the far side and the interaction between speed and flow rate was significant. This was traced to a significant reduction in CV at 30 m/s (*Fig. 9*).

For configuration (c), the symmetry in the coverage pattern was nearly as good as for configuration (b) (*Figs 10 & 7* respectively) except on the far side where the profile was closer to the ones observed for configuration (a) (*Fig. 4*). For configuration (c), both airflow rate and air speed had a significant effect ($P<0{\cdot}05$) on corrected coverage in the centre and on the sprayer side (*Fig. 11*) and only air speed was a significant factor on the far side. The airflow balance was not a significant factor and there was no interaction. On the sprayer side, coverage increased with specific airflow rate at high air speed and with airspeed for high specific airflow rate. In the centre, coverage increased with air speed at low specific airflow rate and 30–70 flow balance and with specific airflow rate at high air speed and 40–60 flow balance. On the far side, coverage

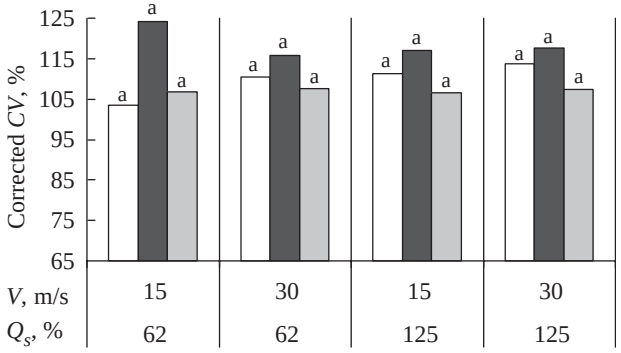

Fig. 6. Coefficient of variation (CV) of coverage for configuration (a); different letters in chart represent significantly different corrected CV within a single canopy location [least significant difference (LSD), probability $P<0{\cdot}05$]; V, air speed; Q_s, specific airflow rate; □, sprayer side; ■, centre; ■, far side

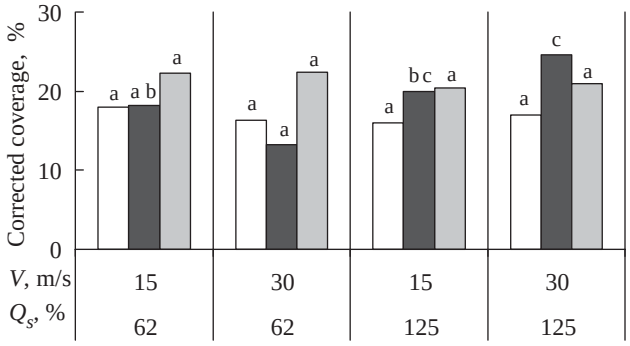

Fig. 8. Mean coverage results for configuration (b); different letters in chart represent significantly different corrected coverage within a single canopy location [least significant difference (LSD), probability $P<0{\cdot}05$]; V, air speed; Q_s, specific airflow rate; □, sprayer side; ■, centre; ■, far side

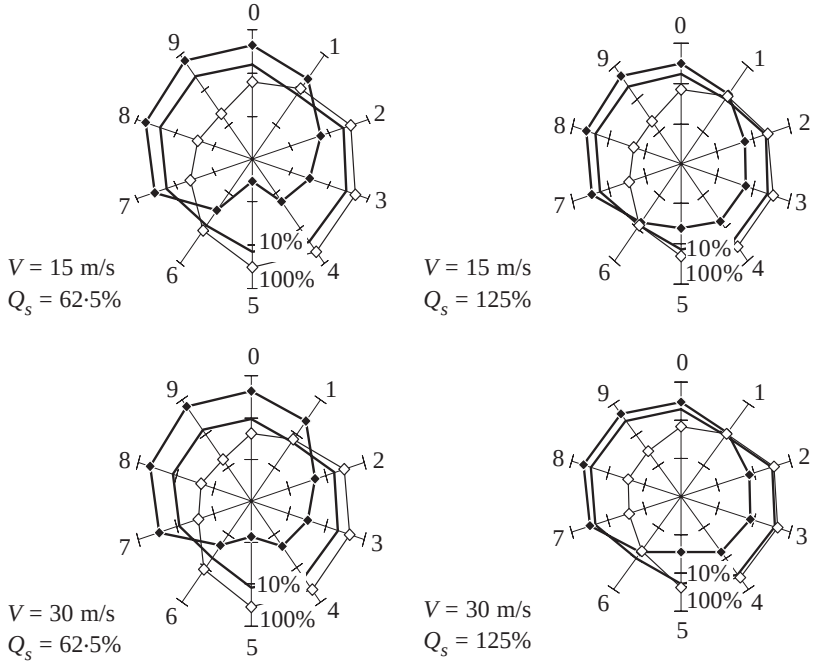

Fig. 7. Polar plots of coverage for configuration (b); V, air speed; Q_s, specific airflow rate; —, centre; —◆—, far side; —◇—, sprayer side

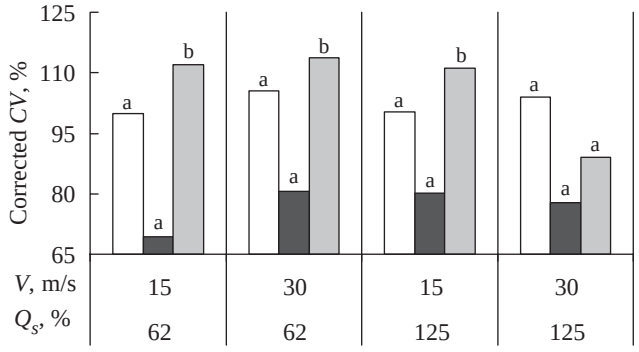

Fig. 9. Coefficient of variation (CV) of coverage for configuration (b); different letters in chart represent significantly different corrected CV within a single canopy location [least significant difference (LSD), probability $P<0{\cdot}05$]; V, air speed; Q_s, specific airflow rate; □, sprayer side; ■, centre; ■, far side

increased with air speed at low specific airflow rate and 30–70 flow balance. When significant differences occurred, increasing airflow rate or air speed increased coverage. Coverage uniformity was improved by increasing specific airflow rate at high air speed on the sprayer side and on the far side by increasing air speed at high specific airflow rate (*Fig. 12*).

The three configurations were compared. For each configuration, the values of the independent variables associated with significantly better coverage were selected pooling the data where appropriate. For configuration (a) and (b), the 125% flow rate was retained pooling data at the two air speeds. For configuration (c), the data were pooled over flow balance at 125% flow rate and 30 m/s air speed. The resulting data set is presented in *Figs 13* and *14*. Configurations were compared for a fixed location using a LSD test (Unistat, 2002). On the far side, corrected coverage from configuration (b) was significantly lower than for configuration (c) and corrected coverage for configuration (a) was not significantly different than the one for either configuration (b) or (c). In the centre, corrected coverage for configurations (b) and (c) was similar and significantly higher than with configuration (a). On the sprayer side, the coverage from all configurations were significantly different. As expected, configuration (b) produced the more uniform coverage across the vine but overall, configuration (c) produced higher corrected coverage than configuration (b). In all cases, configuration (a) resulted in higher values of CV (*Fig. 14*). On the far side, CV for configuration (b) was significantly smaller than CV for configuration (a). In the centre, configurations (b) and (c) had similar CV, both significantly lower than for configuration (a). On the sprayer side, CV for configuration (c) was significantly lower. Again, configuration (b) resulted in a symmetrical pattern of CV across the vine but configuration (c) was slightly better.

It was not expected for configuration (c) to outperform configuration (b). It was first thought that a symmetrical layout of the air sleeves and air-droplet separators would yield better results. It has been pointed out that in configuration (b), the interaction between the two air jets was minimal. This was based on coverage results (*Fig. 7*) and visual observations during the experiments supported this conclusion. With configuration (c), the flow field was more complex as the two air jets interacted strongly. The resulting turbulence is the most probable explanation for the good coverage results that were obtained. It was noted in the discussion of configuration (a), that the surfaces facing away from the coming flow were not well covered. These observations supports the idea that improved coverage can only be obtained by multiplying the number of angle of attack of the flow with respect to any given target surface. This could be achieved either by using multiple air jets or by creating a turbulent flow with a characteristic length scale larger than the size of the target surfaces.

Configuration (c) was easier to implement than configuration (b) as only an air sleeve and a short wet boom had to be supported by the over-the-row structure. Observations during field experiments have revealed that the design of the air-droplet separator while adequate for configuration (a) and (b), was not suitable for configuration (c) as a large portion of the flow did escape in the space between the vine and the separator at the trailing edge. Shifting the separator towards the back of the sprayer and using flaps at the trailing edge to close the gap between the vine and the separator would partly solve the problem.

4. Conclusion

Three configurations for a spray recovery sprayer using air-assistance were tested on vine. In the three cases, a vertical sleeve was used to generate a two-dimensional horizontal air jet of uniform velocity profile from top-to-bottom. The first configuration used a single air jet perpendicular to the row. The second configuration used a pair of air jets, one on each side of the row. Both jet axes were parallel and angled at 33° from the perpendicular to the row. The jet dimension and initial velocity were the same. The separation between these two jets was large enough to avoid any significant interaction. In the third configuration, a first air jet was on one side of the row with its axis perpendicular to the row and a second air jet was on the other side of the vine with its axis intersecting the

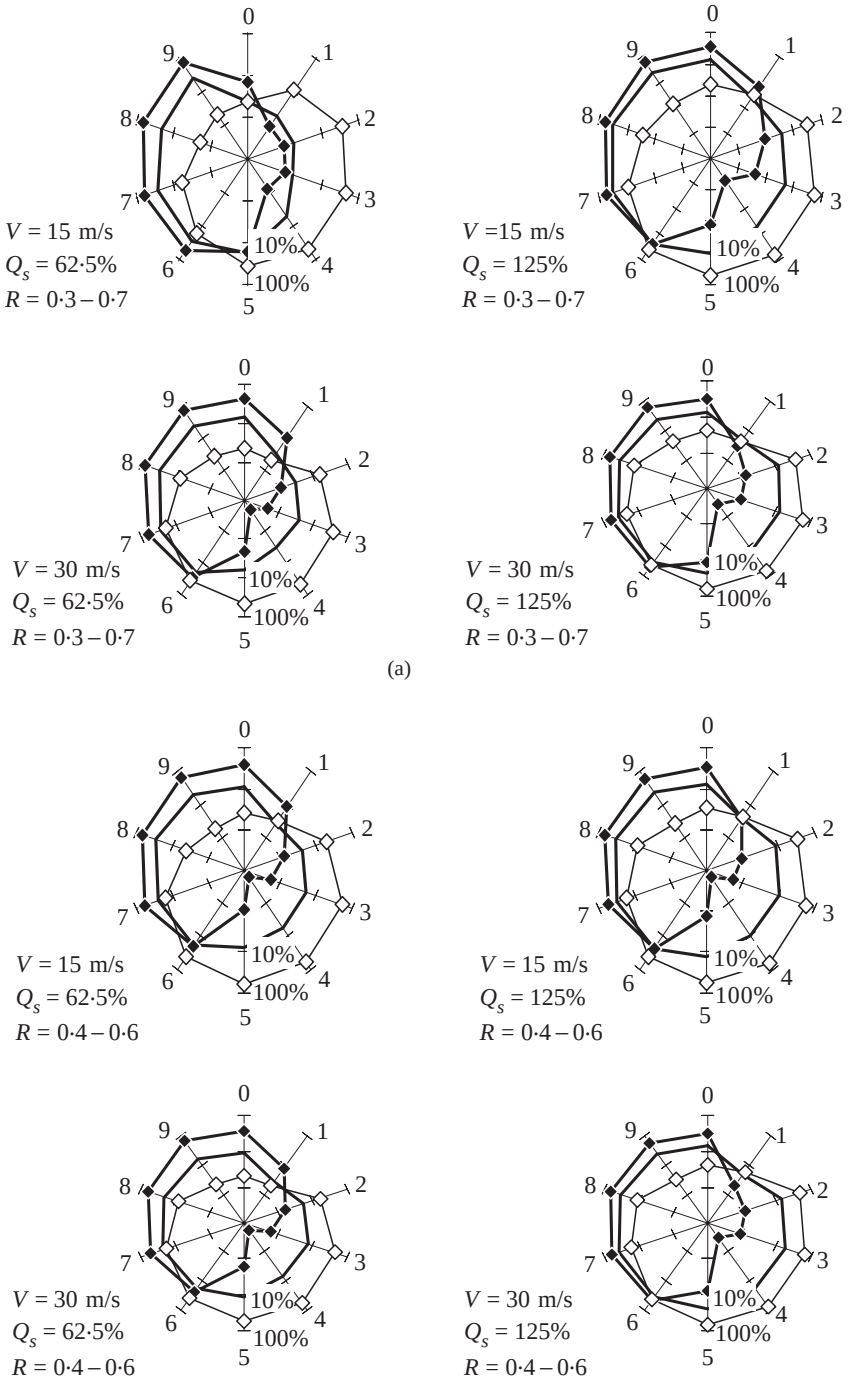

Fig. 10. Polar plots of coverage for configuration (c): (a) 0·3–0·7 flow balance; (b) 0·4–0·6 flow balance; V, air speed; Q_s, specific airflow rate; R, ratio of flow balance; —, centre; —◆—, far side; —◇—, sprayer side

axis of the first jet in the centre of the row. This second air jet delivered a lower flow rate at the same initial speed than the first jet. Results have shown that coverage on artificial cylindrical targets was maximised with the third configuration where a strong interaction between the two jets did occur. Furthermore, the coverage was locally more uniform with this third configuration as with the configuration with two non-interacting jets. These experimental results showed that interacting air jets improved the distribution of the

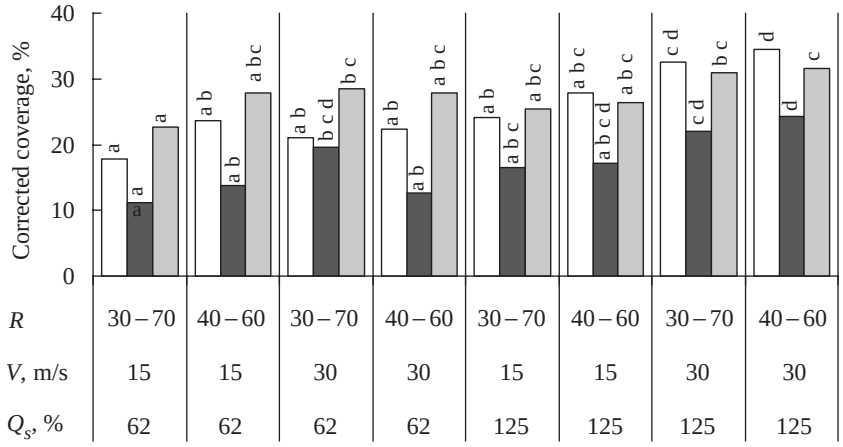

Fig. 11. Mean coverage results for configuration (c); different letters in chart represent significantly different corrected coverage within a single canopy location [least significant difference (LSD), probability $P<0{\cdot}05$]; V, air speed; Q_s, specific airflow rate; □, sprayer side; ■, centre; ■, far side

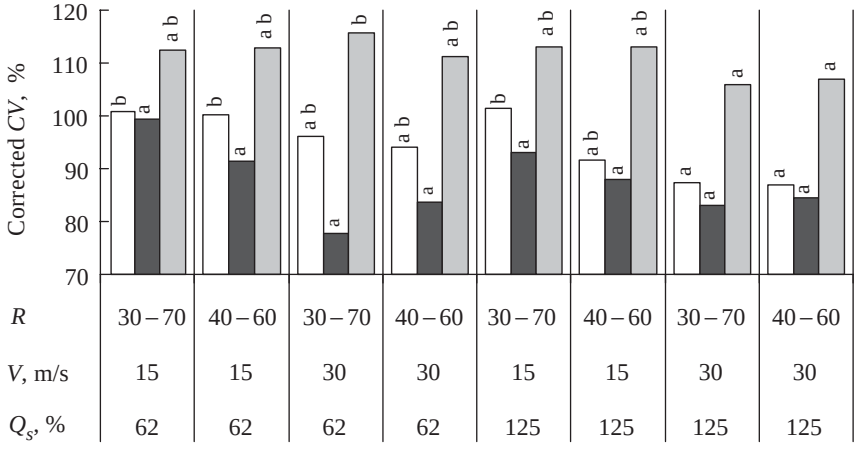

Fig. 12. Coefficient of variation (CV) of coverage for configuration (c); different letters in chart represent significantly different corrected CV within a single canopy location [least significant difference (LSD), probability $P<0{\cdot}05$]; V, air speed; Q_s, specific airflow rate; □, sprayer side; ■, centre; ■, far side

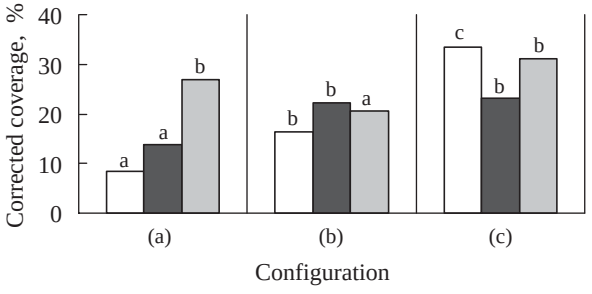

Fig. 13. Mean coverage results for the three configurations under their relative best settings; different letters in chart represent significantly different corrected coverage within a single canopy location [least significant difference (LSD), probability $P<0{\cdot}05$]; □, sprayer side; ■, centre; ■, far side

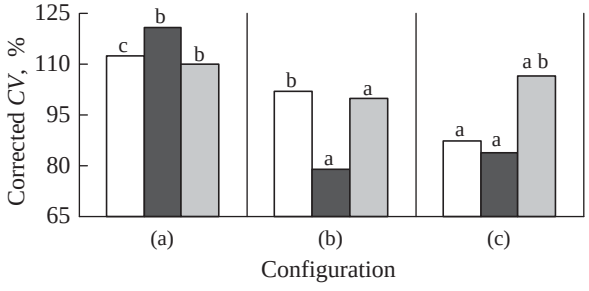

Fig. 14. Coefficient of variation (CV) of coverage for the three configurations under their relative best settings; different letters in chart represent significantly different corrected CV within a single canopy location [least significant difference (LSD), probability $P<0{\cdot}05$]; □, sprayer side; ■, centre; ■, far side

spray within the vine canopy. The improvement in coverage resulted mainly from having a flow coming from widely different directions. In addition, turbulence generated during interactions between air jets might have contributed in improving deposition uniformity on the cylindrical targets.

Acknowledgements

This research was supported by the program PPFI of Agriculture and Agri-Food Canada with the collaborators Ferme Au Pic and the vineyard l'Orpailleur. The authors wish to thank M. Gilles St-Laurent for his contribution to this work.

References

AMCA (1990). Field performance measurement of fan systems. Publication 203-90, doi:6M-012-96P

Abramovich G N (1963). The Theory of Turbulent Jets. MIT Press, Cambridge, MA

ASAE (2000). Spray nozzles classification by droplet spectra. ASAE Standard S572 AUG99

Cross J V; Walklate P J; Murray R A; Richardson G M (2003). Spray deposits and losses in different sized apple trees from an axial fan orchard sprayer, 3: effects of air volumetric flow rate. Crop Protection, **22**(2), 381–394

Doruchowski G; Holownicki R; Godyn A (1997). Effect of spray emission system and air-jet setting on deposit and loss of spray in apple orchard. Journal of Fruit and Ornemental Plant Research, **3**(4), 145–156

Doruchowski G; Svensson S A; Nordmark L (1996). Deposit and loss of spray in orchard as affected by spray discharge system and air jet setting. Acta Horticulturae, **422,** 383–384

Furness G O; Pinczewski W V (1985). A comparison of the spray distribution obtained from sprayers with converging and diverging airjets with low volume air assisted spraying on citrus and grapevines. Journal of Agricultural Engineering Research, **32,** 291–310

Gohlich H (1985). Deposition and penetration of sprays. Symposium on Application and Biology—BCPC Monogram No. 28, pp 173–182

Holownicki R; Doruchowski G; Godyn A; Swiechowski W (2002). The effect of air jet velocity on spray deposit in an apple orchard. Aspects of Applied Biology, **66,** 277–283

Matthews G A (2000a). A review of the use of air in atomisation of sprays, dispersion of droplets down wind and collection on crop foliage. Aspects of Applied Biology, **57,** 21–27

Matthews G A (2000b). Pesticide Application Methods, 3rd Edn. Blackwell Science, Oxford, UK

Neter J; Wasserman W; Kutner M H (1990). Applied Linear Statistical Models, 3rd Edn. Irwin, Boston

Panneton B (2002). Image analysis of water-sensitive cards for spray coverage experiments. Applied Engineering in Agriculture, **18**(2), 179–182

Panneton B; Thériault R; Lacasse B (2001). Efficacy evaluation of a new spray-recovery sprayer for orchards. Transactions of the ASAE, **44**(3), 473–479

Pergher G; Gubiani R (1995). The effect of spray application rate and airflow rate on foliar deposition in a hedgerow vineyard. Journal of Agricultural Engineering Research, **61,** 205–216

Pergher G; Gubiani R; Tonetto G (1997a). Foliar deposition and pesticide losses from three air-assisted sprayers in a hedgerow vineyard. Crop Protection, **16**(1), 25–33

Pergher G; Gubiani R; Tonetto G (1997b). Foliar deposition and pesticide losses from three air-assisted sprayers in a hergerow vineyard. Crop Protection, **16**(1), 25–33

Pezzi F; Rondelli V (2000). The performance of an air-assisted sprayer operating in vines. Journal of Agricultural Engineering Research, **76,** 331–340

Randall J M (1971). The relationships between air volume and pressure on spray distribution in fruit trees. Journal of Agricultural Engineering Research, **16**(1), 1–31

Spillman J J (1987). Improvements required in spray droplet formation to improve application technology. Symposium on the Aerial Application of Pesticide in Forestery, Ottawa, Canada, pp 37–42

Stafford E M; Byass J B; Akesson N B (1970). A fluorescent pigment to measure spray coverage. Journal of Economic Entomology, **63**(3), 769–776

Unistat (2002). Unistat® 5.5 Statistical Package for Windows—User's Guide. Unistat Ltd, London, UK

Viret O; Siegfried W; Holliger E; Raisigl U (2003). Comparison of spray deposits and efficacy against powdery mildew of aerial and ground-based spraying equipment in viticulture. Crop Protection, **22**(8), 1023–1032